IEEE Access
Multidisciplinary ⋮ Rapid Review ⋮ Open Access Journal

Received 4 July 2024, accepted 10 July 2024, date of publication 15 July 2024, date of current version 23 July 2024.

Digital Object Identifier 10.1109/ACCESS.2024.3428341

RESEARCH ARTICLE

Robust Adaptive Heterogeneous Vehicle Platoon Control Based on Disturbances Estimation and Compensation

FERNANDO VIADERO-MONASTERIO, (Member, IEEE),
MIGUEL MELÉNDEZ-USEROS, (Graduate Student Member, IEEE),
MANUEL JIMÉNEZ-SALAS, (Graduate Student Member, IEEE),
AND BEATRIZ L. BOADA
Mechanical Engineering Department, Advanced Vehicle Dynamics and Mechatronic Systems (VEDYMEC), Universidad Carlos III de Madrid, 28911 Leganés, Spain

Corresponding author: Fernando Viadero-Monasterio (fviadero@ing.uc3m.es)

This work was supported in part by MCIN/AEI/10.13039/501100011033 under Grant PID2022-136468OB-I00, and in part by "the European Regional Development Fund (ERDF) A Way of Making Europe."

ABSTRACT This paper presents an investigation into the problem of controlling a heterogeneous vehicle platoon, focusing on two aspects: the impact of noise in sensor measurements and the effect of road slope, wind, and rolling resistance on the longitudinal dynamics of each vehicle. To maintain an adequate separation between each follower, a static output feedback (SOF) controller is designed within the predecessor-leader-follower vehicle platoon topology. In order to mitigate the impact of sensor measurement noise and external disturbances on the system, robust control theory is incorporated into the controller design. The engine's control input is adjusted to compensate for external road disturbances affecting the longitudinal dynamics of each vehicle. This estimation is achieved through the use of a Kalman filter. Closed-loop stability of the heterogeneous vehicle platoon is ensured through a Lyapunov functional analysis. Simulations have shown that the proposed methodology achieves smoother platoon following than a strategy that does not consider or compensate the effect of disturbances on the longitudinal dynamics of the vehicle.

INDEX TERMS Disturbances, heterogeneous vehicle platoon, longitudinal dynamics, platoon control, robust control.

I. INTRODUCTION

Vehicular platoon control has emerged as a subject of intense research and development due to its potential to revolutionize the transportation industry. One of the primary motivations driving the interest in vehicular platooning is its capability to significantly enhance road safety [1]. The use of automated driving systems (ADS) enables precise control and coordination among vehicles, virtually eliminating human errors such as distracted driving, fatigue, or recklessness [2], [3], [4]. It is anticipated that the collective intelligence and enhanced situational awareness resulting from the implementation of autonomous vehicle platoons will lead to a reduction in the likelihood of accidents, thereby improving road safety and reducing casualties [5]. Moreover, vehicular platooning offers a viable solution for tackling the growing problem of traffic congestion [6]. By maintaining consistent inter-vehicle distances and synchronized speeds, platoons can improve traffic flow and reduce the inefficiencies caused by stop-and-go driving [7].

Vehicle platooning, despite its many potential benefits, also faces several technical challenges [8]. Implementing vehicle platooning requires advanced technologies, including vehicle-to-vehicle communication (V2V), sensor systems, and sophisticated control algorithms [9], [10]. Concerning the communication of the vehicles in the platoon, the

The associate editor coordinating the review of this manuscript and approving it for publication was Jinquan Xu.

predecessor-leader follower (PLF) is the most common topology [11]. PLF has a clear advantage compared to predecessor follower (PF) topology, since constant spacing cannot be maintained together with string stability in PF [12]. Furthermore, the PF topology exhibits a delayed reaction time to changes in the platoon's status, as it lacks information about the leader's states. Although PF is a mature technique and is implemented in series-production vehicles through adaptive cruise control (ACC) [13], there is still a large amount of research to be done for PLF. In PLF, the leading vehicle periodically transmits its states, such as position, velocity and acceleration to each vehicle in the platoon, while every follower is able to obtain relative information to the predecessor vehicle with RADAR or LiDAR sensors [14].

Another significant problem is the control of heterogeneous vehicle platoons, which integrate and coordinate vehicles with different mechanical properties and dimensions [15], [16], [17]. Although there is extensive research on homogeneous vehicle platoon control [18], [19], [20], [21], [22], it limits its practical application as every vehicle in the platoon must be identical. To simulate real-world scenarios, it is recommended to use a heterogeneous platoon model for the controller design, which is more robust due to the fact that each vehicle may have different specifications [23], [24], [25].

External disturbances such as wind, rolling resistance and road slope affect the longitudinal dynamic behavior of the vehicle [26], however, it is common in the literature for many researchers to neglect this phenomenon [18], [27]. There are several works that include this effect on the dynamic model of the platoon [28], [29], [30], [31]. In [30], a radial basis function neural network is considered to estimate uncertainties in vehicle parameters. In [31], an extended Kalman filter (EKF) is used to estimate the road slope, however it does not consider the effect of wind or rolling resistance.

To design the platoon controller that generates the input signal to the engine, there are several alternatives. In [27], a model predictive control (MPC) is proposed for connected vehicle platoon with a focus on switching communication topologies and control strategy under abnormal communications. The problem with MPC techniques is that they require either an expensive computational burden for real-time implementation when using online MPCs or fine parameter tuning for offline MPCs, which leads to difficulties when deploying these on real systems [32], [33], [34]. Moreover, full-state knowledge is needed for MPC, which is not always possible in practice [35]. In [36], a resilient platoon control considering attacks on the communication is studied. However, it is applied on a homogeneous platoon and the effect of road slope, wind and rolling resistance is not analyzed. In addition, none of these works consider sensor noise. To achieve a good tradeoff against the effect of external disturbances on the vehicle, robust control is frequently utilized. $\mathscr{H}_\infty$ is one of the preferred robust control techniques amongst researchers, since it minimizes the closed loop impact of a perturbation, bounding the maximum transitivity to the system in any frequency [37], [38], [39]. In [40], a robustness analysis of heterogeneous platoon switching control under bounded disturbance is presented, and sufficient conditions for $\mathscr{L}_2$ string stability are provided. In [41], a decoupled $\mathscr{H}_\infty$ control method for automated vehicular platoon to comprehensively compromise multiple performances is presented. However, none of the aforementioned works consider sensor noise for the controller design.

Motivated by the aforementioned reasons, a robust heterogeneous vehicle platoon controller with disturbance estimation and compensation is investigated in this work. The main contributions of this paper are:

- As the vehicles do not have access to the full platoon states (since predecessor leader follower topology is chosen), a static output feedback (SOF) controller is designed for each vehicle. This controller generates an acceleration command based on relative measurements to the predecessor and leader vehicle. In order to solve the non-convex problem of output feedback control, LMI conditions are derived.
- In order to deal with sensor noise, a platoon controller has been designed following robust control techniques that minimize the closed-loop impact of sensor errors over the platoon.
- The longitudinal platoon dynamics are affected by road slope, wind, and rolling resistance. To correct the necessary control input to each vehicle engine, their combined effect on each vehicle is estimated using a Kalman filter.

The rest of this article is organized as follows. In Section II, a modelling for the heterogeneous vehicle platoon problem is presented. In Section III, the proposed robust heterogeneous vehicle platoon controller design is explained, amongst the stability analysis of the closed-loop system. In Section IV, an estimator is designed to analyze the effect of external disturbances over the longitudinal dynamics of the vehicle. The validity of this study is proven in Section V. Finally, the conclusions of the article are provided in Section VI.

Notation. The set of nonnegative integers is denoted by $\mathbb{Z}_+$. For a matrix X, $X^\top$ denotes its transpose. If Y is a square matrix, $Y > 0$ denotes that Y is positive definite. In a symmetric matrix, the symbol $\star$ indicates the transpose of the symmetric term. The function $diag\left\{X_1, X_2\right\}$ retrieves a block-diagonal matrix composed by X_1 and X_2. If not stated, matrices are supposed to have compatible dimensions. $\mathscr{N}(\mu, \sigma)$ denotes a Gaussian distribution with mean μ and standard deviation σ. Arguments are omitted when their meaning is clear.

II. HETEROGENEOUS VEHICLE PLATOON MODELING

This section presents a description of the longitudinal dynamics of a heterogeneous vehicle platoon model. Consider a heterogeneous vehicle platoon with a leader and n following

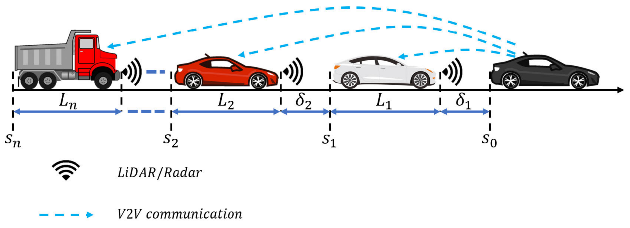

FIGURE 1. **Heterogeneous vehicle platoon with PLF communication.**

vehicles as is depicted in **Figure** 1. s_i, v_i and a_i denote the ith vehicle's position, velocity and acceleration, respectively; with $i = 0$ representing the leader and $i = 1, \ldots, n$ reflecting the ith follower.

In a heterogeneous vehicle platoon that follows the PLF topology, the leader vehicle periodically transmits its status, such as position, velocity and acceleration to each follower in the platoon through a wireless network. These states can be obtained from a variety of sensors. GPS, odometers and accelerometers are viable options, as they are already included in most modern production vehicles. Additionally, follower vehicles are equipped with sensors such as LiDAR or Radar that measure the relative distance, speed, and acceleration with respect to the preceding vehicle.

One of the main purposes of vehicular platoons is to improve traffic flow by maintaining adequate spacing between vehicles. The present paper adopts a constant spacing policy, since it enables platoons with small inter-vehicle distances, resulting in improved fuel efficiency, and increased traffic throughput [7], [12]. The spacing error of the ith following vehicle is defined as

$$\delta_i(t) = s_{i-1}(t) - s_i(t) - \delta_d - L_i \tag{1}$$

where δ_d is the desired spacing between consecutive vehicles and L_i is the ith vehicle length. The spacing error dynamics (speed and acceleration errors) are described by:

$$\begin{aligned} \dot{\delta}_i(t) &= \dot{s}_{i-1}(t) - \dot{s}_i(t) = v_{i-1}(t) - v_i(t) \\ \ddot{\delta}_i(t) &= \dot{v}_{i-1}(t) - \dot{v}_i(t) = a_{i-1}(t) - a_i(t) \end{aligned} \tag{2}$$

The acceleration is dependent on the longitudinal dynamic behaviour of the ith vehicle, which is described by the following non-linear model [42]:

$$\dot{a}_i(t) = -\frac{a_i(t)}{\tau_i} - \frac{d_i(t)}{\tau_i} + \frac{c_i(t)}{\tau_i m_i} \tag{3}$$

where c_i is the traction force exerted by the vehicle, d_i denotes the combined effect of external disturbances that affect the longitudinal vehicle dynamics: the aerodynamics drag, rolling resistance and gravitational resistance. The function $d_i(t)$ is expressed as:

$$\begin{aligned} d_i(t) = &\frac{0.5\rho C_{wi} \Lambda_i \big(v_i(t) - v_w(t)\big)^2}{m_i} \\ &+ g\big(f_{ri}\cos\theta_i(t) + \sin\theta_i(t)\big) \end{aligned} \tag{4}$$

where $\rho = 1.293\ kg/m^3$ is the air density and $g = 9.81\ m/s^2$ the gravitational constant acceleration. The main parameters for typical passenger vehicles are described in **Table** 1.

To implement the control law, we perform the following variable change:

$$u_i(t) = -d_i(t) + \frac{c_i(t)}{m_i} \tag{5}$$

which leads to the linearized system:

$$\dot{a}_i(t) = -\frac{a_i(t)}{\tau_i} + \frac{u_i(t)}{\tau_i} \tag{6}$$

Remark 1: In (6), u_i is an input signal that simplifies the system model by combining the effects of traction force and external disturbances that affect the longitudinal dynamics of the vehicle. The controller that generates this signal is presented in **Section** III. In order to undo the change of variable in (5) and determine the traction force c_i to apply on the ith vehicle, it is required to track the combined effect of external disturbances (aerodynamic drag, rolling and gravitational resistances). An estimator is proposed in **Section** IV in order to accomplish this.

In order to achieve a compact heterogeneous vehicle platoon model, the tracking error ξ_i between the leader and each follower is used:

$$\begin{aligned} \xi_i(t) &= s_0(t) - s_i(t) - \overline{L}_i - \overline{\delta}_{d,i} \\ \dot{\xi}_i(t) &= v_0(t) - v_i(t) \\ \ddot{\xi}_i(t) &= a_0(t) - a_i(t) \\ \dddot{\xi}_i(t) &= \dot{a}_0(t) - \left(-\frac{a_i(t)}{\tau_i} + \frac{u_i(t)}{\tau_i}\right) \\ &= \dot{a}_0(t) + \frac{a_i(t)}{\tau_i} - \frac{u_i(t)}{\tau_i} \\ &= \left(\dot{a}_0(t) + \frac{a_0(t)}{\tau_i}\right) \\ &\quad - \left(\frac{a_0(t)}{\tau_i} - \frac{a_i(t)}{\tau_i}\right) - \frac{u_i(t)}{\tau_i} \\ &= \mathcal{B}_{di}\omega(t) - \frac{\ddot{\xi}(t)}{\tau_i} - \frac{u_i(t)}{\tau_i} \end{aligned} \tag{7}$$

where the model disturbance is denoted as ω

$$\omega(t) = \begin{bmatrix} \dot{a}_0(t) & a_0(t) \end{bmatrix}^\top, \quad \mathcal{B}_{di} = \begin{bmatrix} 0 & 0 & 1 \\ 0 & 0 & \frac{1}{\tau_i} \end{bmatrix}^\top \tag{8}$$

moreover, $\overline{L}_i$ is the sum of all vehicles' length between the leader and the ith follower and $\overline{\delta}_{d,i}$ is the ideal vehicle spacing between the leader and ith follower. These parameters are calculated as follows:

$$\overline{L}_i = \sum_{j=1}^{i} L_j, \quad \overline{\delta}_{d,i} = \sum_{j=1}^{i} \delta_d \tag{9}$$

Following the tracking error ξ_i presented in (7) and the effect of the model disturbance ω from (8), the longitudinal

TABLE 1. **Minimum and maximum limits of vehicle parameters and external disturbances [43], [44].**

Symbol	Description	Unit	Min.	Max.
m_i	Vehicle mass	kg	800	2000
τ_i	Time constant of powertrain dynamics	s	0.2	0.8
C_{wi}	Coefficient of aerodynamic drag	–	0.29	0.39
Λ_i	Frontal cross-area	m^2	1.58	2.9
f_{ri}	Coefficient of rolling resistance	–	0.01	0.014
v_w	Wind speed	m/s	-12.9	12.9
θ_i	Road slope	°	-17.0[a] -5.9[b]	17.0[a] 5.9[b]

[a] *Hilly road*

[b] *Highway & expressway*

behavior of the ith vehicle (7) follows the continuous state-space dynamics:

$$\dot{\zeta}_i(t) = \mathcal{A}_i\zeta_i(t) + \mathcal{B}_i u_i(t) + \mathcal{B}_{di}\omega(t) \tag{10}$$

where

$$\zeta_i(t) = \begin{bmatrix} \xi_i(t) \\ \dot{\xi}_i(t) \\ \ddot{\xi}_i(t) \end{bmatrix}, \; \mathcal{A}_i = \begin{bmatrix} 0 & 1 & 0 \\ 0 & 0 & 1 \\ 0 & 0 & -\frac{1}{\tau_i} \end{bmatrix}, \; \mathcal{B}_i = \begin{bmatrix} 0 \\ 0 \\ -\frac{1}{\tau_i} \end{bmatrix}$$

III. ROBUST STATIC OUTPUT FEEDBACK CONTROLLER DESIGN FOR A HETEROGENEOUS VEHICLE PLATOON

This section presents the design of a static output feedback controller for a heterogeneous vehicle platoon. The controller must be robust against external disturbances and measurement noise, and stable under Lyapunov criteria. To find a feasible solution, Linear Matrix Inequality (LMI) conditions are derived.

A. CONTROLLER DESIGN

The objective of the platoon controller is to generate a reference acceleration command based on relative information about the leader and the preceding vehicle so that each vehicle follows the platoon with the lowest spacing error. The control input u_i is generated as follows:

$$\begin{aligned} u_i = \; & k_{i1}(\tilde{s}_{i-1} - \tilde{s}_i - \delta_d - L_i) \\ & + k_{i2}(\tilde{v}_{i-1} - \tilde{v}_i) + k_{i3}(\tilde{a}_{i-1} - \tilde{a}_i) \\ & + k_{i4}(\tilde{s}_0 - \tilde{s}_i - \overline{L}_i - \overline{\delta}_{d,i}) \\ & + k_{i5}(\tilde{v}_0 - \tilde{v}_i) + k_{i6}(\tilde{a}_0 - \tilde{a}_i) \end{aligned} \tag{11}$$

where k_{ij} ($i = 1, \ldots, n, j = 1, \ldots, 6$), are the control gains to design.

Remark 2: The symbol $\sim$ in (11) is used to indicate the measurement obtained from the sensors, which will never correspond to the exact value of the states, due to the presence of noise. In order to deal with measurement noise, a robust controller is to be designed through this section.

By substituting (7) in (11), the control law for the ith follower is rewritten as:

$$\begin{aligned} u_i = \; & k_{i1}(\tilde{\xi}_i - \tilde{\xi}_{i-1}) + k_{i2}(\dot{\tilde{\xi}}_i - \dot{\tilde{\xi}}_{i-1}) \\ & + k_{i3}(\ddot{\tilde{\xi}}_i - \ddot{\tilde{\xi}}_{i-1}) + k_{i4}\tilde{\xi}_i + k_{i5}\dot{\tilde{\xi}}_i + k_{i6}\ddot{\tilde{\xi}}_i \end{aligned} \tag{12}$$

Applying the changes of variable

$$\begin{aligned} \begin{bmatrix} k_{i1} & k_{i2} & k_{i3} \end{bmatrix} &= M_{i1}N_{i1}^{-1} \\ \begin{bmatrix} k_{i4} & k_{i5} & k_{i6} \end{bmatrix} &= M_{i2}N_{i2}^{-1} \end{aligned} \tag{13}$$

the control input for each vehicle is implemented with a static output feedback controller (SOFC):

$$u_i(k) = M_{i1}N_{i1}^{-1}(\tilde{\zeta}_{i-1}(k) - \tilde{\zeta}_i(k)) + M_{i2}N_{i2}^{-1}\tilde{\zeta}_i(k) \tag{14}$$

In order to facilitate real-time implementation, the platoon control design is performed in the discrete time domain. Now system (10) is transformed into its discrete-time counterpart via Euler's discretization:

$$\zeta_i(k+1) = A_i\zeta_i(k) + B_i u_i(k) + B_{di}\omega(k) \tag{15}$$

The state-space matrices of (15) are given by

$$A_i = I + T_d\mathcal{A}_i, \quad B_i = T_d\mathcal{B}_i, \quad B_{di} = T_d\mathcal{B}_{di}$$

where T_d is the sampling time in seconds.

Expanding (15) to every follower and considering (14), the model of the whole heterogeneous vehicle platoon is defined as

$$\begin{aligned} \zeta(k+1) &= A\zeta(k) + BMN^{-1}C_y\tilde{\zeta}(k) + B_d\omega(k) \\ \tilde{\zeta}(k) &= \zeta(k) + e_y(k) \\ z(k) &= C_z\zeta(k) \end{aligned} \tag{16}$$

where e_y represents the measurement noise and z is the control output to minimize. The system matrices of the augmented model are

$$\begin{aligned} \zeta &= \left[\zeta_i^\top, \ldots, \zeta_n^\top\right]^\top, A = diag\left\{A_1, \ldots, A_n\right\}, \\ B &= diag\left\{\left[B_1 \; B_1\right], \ldots, \left[B_n \; B_n\right]\right\}, \\ B_d &= \left[B_{d1}^\top, \ldots, B_{dn}^\top\right]^\top, \\ M &= diag\left\{M_{11}, M_{12}, \ldots, M_{n1}, M_{n2}\right\}, \\ N &= diag\left\{N_{11}, N_{12}, \ldots, N_{n1}, N_{n2}\right\}, \\ C_y &= \left[C_{11}^\top, C_{12}^\top, \ldots, C_{n1}^\top, C_{n2}^\top\right]^\top, C_z = I, \\ C_{11} &= \left[I \; 0 \ldots 0\right], C_{12} = \left[I \; 0 \ldots 0\right], \\ C_{21} &= \left[-I \; I \; \ldots 0\right], C_{22} = \left[0 \; I \; \ldots 0\right], \\ C_{n1} &= \left[0 \ldots -I \; I\right], C_{n2} = \left[0 \ldots 0 \; I\right] \end{aligned}$$

The following theorem provides sufficient conditions to design a robust SOF controller for the heterogeneous vehicle platoon (16).

Theorem 1: The closed-loop vehicle platoon system (16) is asymptotically stable with an $\mathscr{H}_\infty$ performance index $\gamma > 0$ if there exist a matrix $Q > 0$ and a matrix M such that the following LMI holds

$$\begin{bmatrix} -Q & \star & \star & \star & \star \\ 0 & -\gamma^2 I & \star & \star & \star \\ 0 & 0 & -\gamma^2\gamma_y^2 I & \star & \star \\ AQ+BMC_y & B_d & BMC_y & -Q & \star \\ C_zQ & 0 & 0 & 0 & -I \end{bmatrix} < 0 \tag{17}$$

Once a feasible solution is found, the controller gains are obtained by

$$\begin{aligned} N_{ij}C_{ij} &= C_{ij}Q, \\ \begin{bmatrix} k_{i1} & k_{i2} & k_{i3} \end{bmatrix} &= M_{i1}N_{i1}^{-1}, \\ \begin{bmatrix} k_{i4} & k_{i5} & k_{i6} \end{bmatrix} &= M_{i2}N_{i2}^{-1} \end{aligned} \tag{18}$$

where $i = 1, \ldots, n, j = 1, 2$.

Proof. The discrete-time Lyapunov function is chosen to analyze the system stability

$$\mathcal{V}(k) = \zeta(k)^\top P \zeta(k) \tag{19}$$

with $P > 0$. The closed-loop trajectory of the system (16) is stable if the following condition is satisfied

$$\Delta\mathcal{V}(k) = \mathcal{V}(k+1) - \mathcal{V}(k) < 0 \tag{20}$$

In order to mitigate the effect of model disturbances and measurement noise on the system, $\mathscr{H}_\infty$ criteria is considered

$$z^\top(k)z(k) - \gamma^2\omega(k)^\top\omega(k) - \gamma^2\gamma_y^2\hat{e}_y(k)^\top\hat{e}_y(k) < 0 \tag{21}$$

where γ is the $\mathscr{H}_\infty$ performance index to minimize, γ_y is a weighting factor and $\hat{e}_y$ is obtained through the change of variable

$$\hat{e}_y(k) = Pe_y(k) \tag{22}$$

Combining the Lyapunov stability criteria (20) and the $\mathscr{H}_\infty$ criteria (21) yields the inequation

$$\begin{aligned} \Delta\mathcal{V}(k) + z^\top(k)z(k) - \gamma^2\omega(k)^\top\omega(k) \\ - \gamma^2\gamma_y^2\hat{e}_y(k)^\top\hat{e}_y(k) < 0 \end{aligned} \tag{23}$$

note that (23) can be expressed as the quadratic form

$$\begin{aligned} \begin{bmatrix} \zeta(k) \\ \omega(k) \\ \hat{e}_y(k) \end{bmatrix}^\top \left(\begin{bmatrix} -P+C_z^\top C_z & \star & \star \\ 0 & -\gamma^2 I & \star \\ 0 & 0 & -\gamma^2\gamma_y^2 I \end{bmatrix} \right. \\ \left. + \Gamma^\top P \Gamma \right) \begin{bmatrix} \zeta(k) \\ \omega(k) \\ \hat{e}_y(k) \end{bmatrix} < 0 \end{aligned} \tag{24}$$

where

$$\Gamma = \begin{bmatrix} A+BMN^{-1}C_y & B_d & BMN^{-1}C_yP^{-1} \end{bmatrix}$$

Being (24) a quadratic form, its negativity depends solely on the eigenvalues of the matrix. Therefore, the inequality can be further manipulated by applying the Schur complement, resulting in the following LMI problem

$$\begin{bmatrix} -P+C_z^\top C_z & \star & \star & \star \\ 0 & -\gamma^2 I & \star & \star \\ 0 & 0 & -\gamma^2\gamma_y^2 I & \star \\ A+BMN^{-1}C_y & B_d & BMN^{-1}C_yP^{-1} & -P^{-1} \end{bmatrix} < 0 \tag{25}$$

Now apply the congruent transformation *diag* $\{P^{-1}, I, I, I\}$ to the LMI (25) to obtain

$$\begin{bmatrix} -P^{-1}+P^{-1}C_z^\top C_zP^{-1} & \star & \star & \star \\ 0 & -\gamma^2 I & \star & \star \\ 0 & 0 & -\gamma^2\gamma_y^2 I & \star \\ AP^{-1}+BMN^{-1}C_yP^{-1} & B_d & BMN^{-1}C_yP^{-1} & -P^{-1} \end{bmatrix} < 0 \tag{26}$$

Finally, perform the changes of variable $P^{-1} = Q$ and (18). After applying the Schur complement, the LMI (26) becomes (17), hence the proof is complete. ☐

B. STRING STABILITY ANALYSIS

The following theorem gives sufficient conditions to ensure the string stability of the heterogeneous vehicle platoon (16).

Theorem 2: If the LMI (17) retrieves a feasible solution, the PLF feedback gains $k_j, j = 1, \ldots, 5$ can guarantee that the closed-loop heterogeneous vehicle platoon (16) is string stable. Moreover, if $0 < \gamma < 1$, then the platoon is strictly string stable.

Proof. The proof is found in [28] and [29] and is omitted here for simplicity.

IV. LONGITUDINAL VEHICLE DYNAMIC DISTURBANCES ESTIMATION AND COMPENSATION BASED ON KALMAN FILTER

This section presents the design of a Kalman filter to estimate the impact of external disturbances on the longitudinal dynamics of each vehicle in the platoon. The effect of these disturbances is later compensated by updating the control input as follows:

$$c_i = u_i m_i + \hat{d}_i m_i \tag{27}$$

where $\hat{d}_i$ denotes the estimated external disturbances for the ith vehicle. To perform the estimation, the following sub-model is considered for each vehicle of the platoon:

$$\dot{x}_i(t) = \mathcal{F}_i x_i(t) + \mathcal{G}_i u_i(t) + \mathcal{G}_{d,i} d_i(t) \tag{28}$$

where

$$x_i(t) = \begin{bmatrix} s_i(t) \\ v_i(t) \\ a_i(t) \end{bmatrix}, \qquad \mathcal{F}_i = \begin{bmatrix} 0 & 1 & 0 \\ 0 & 0 & 1 \\ 0 & 0 & -\frac{1}{\tau_i} \end{bmatrix},$$

$$\mathcal{G}_i = \begin{bmatrix} 0 \\ 0 \\ \frac{1}{\tau_i} \end{bmatrix}, \qquad \mathcal{G}_{d,i} = \begin{bmatrix} 0 \\ 0 \\ -\frac{1}{\tau_i} \end{bmatrix}$$

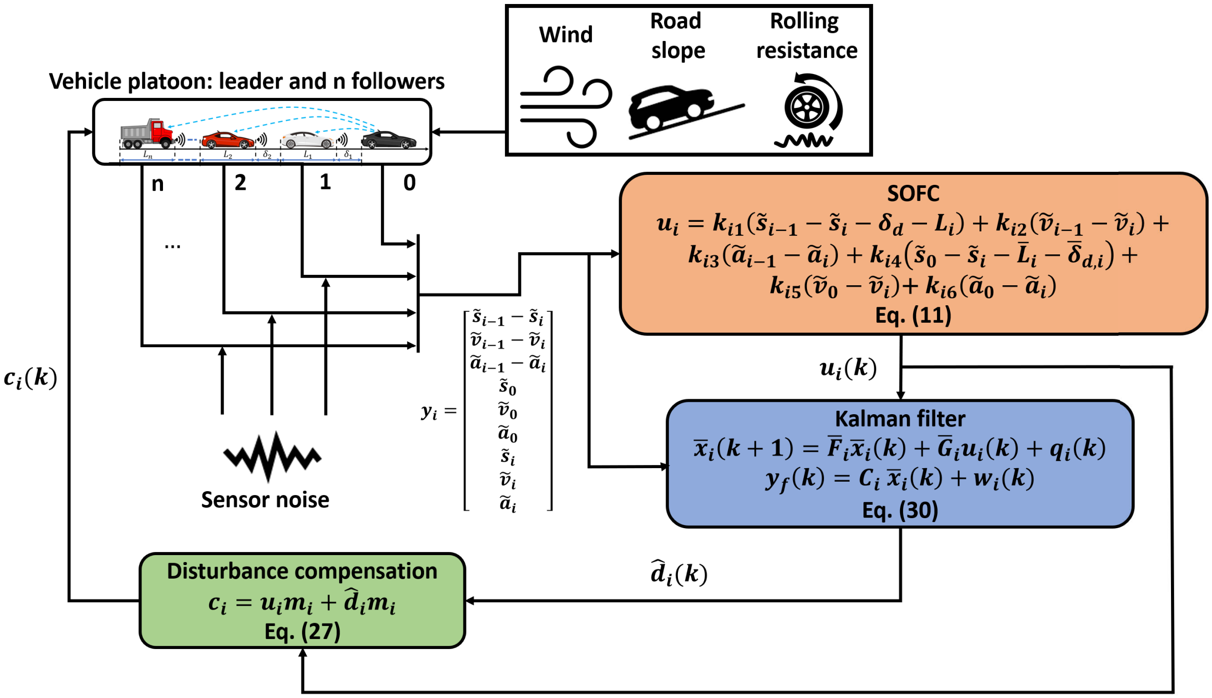

FIGURE 2. Proposed control architecture for the heterogeneous vehicle platoon.

System (28) is expanded in order to consider external disturbances as a state

$$\dot{\overline{x}}_i(t) = \overline{\mathcal{F}}_i\overline{x}_i(t) + \overline{\mathcal{G}}_iu_i(t) \tag{29}$$

where

$$\overline{x}_i(t) = \begin{bmatrix} s_i(t) \\ v_i(t) \\ a_i(t) \\ d_i(t) \end{bmatrix}, \quad \overline{\mathcal{F}}_i = \begin{bmatrix} 0 & 1 & 0 & 0 \\ 0 & 0 & 1 & 0 \\ 0 & 0 & -\frac{1}{\tau_i} & -\frac{1}{\tau_i} \\ 0 & 0 & 0 & 0 \end{bmatrix},$$

$$\overline{\mathcal{G}}_i = \begin{bmatrix} 0 \\ 0 \\ \frac{1}{\tau_i} \\ 0 \end{bmatrix}$$

The system is transformed into its discrete analogue via the Euler's discretization:

$$\overline{F}_i = I + T_d\overline{\mathcal{F}}_i, \quad \overline{G}_i = T_d\overline{\mathcal{G}}_i$$

The equations of the Kalman filter to design are:

$$\begin{aligned} \overline{x}_i(k+1) &= \overline{F}_i\overline{x}_i(k) + \overline{G}_iu_i(k) + q_i(k) \\ y_f(k) &= C_i\overline{x}_i(k) + w_i(k) \end{aligned} \tag{30}$$

where

$$C_i = \begin{bmatrix} 1 & 0 & 0 & 0 \\ 0 & 1 & 0 & 0 \\ 0 & 0 & 1 & 0 \end{bmatrix}$$

and the measurements $y_f(k) = \left[s_i(k)\ v_i(k)\ a_i(k)\right]^\top$. q_i and w_i are the process and measurement noise, respectively, defined by the system noise covariance $\mathcal{Q}$ and the measurement noise covariance $\mathcal{R}$:

$$\begin{aligned} q_i(k) &\sim \mathcal{N}(0, \mathcal{Q}) \\ w_i(k) &\sim \mathcal{N}(0, \mathcal{R}) \end{aligned} \tag{31}$$

The design of the Kalman filter can be found in [45] and is omitted here for simplicity.

V. SIMULATION RESULTS

To evaluate the effectiveness of the proposed robust controller, a simulation for a heterogeneous vehicle platoon with a leader and $n = 5$ followers with varying road conditions is conducted using *MATLAB*. The longitudinal vehicle dynamics of the platoon are simulated in accordance with (16). The proposed control architecture for the vehicle platoon is depicted in **Figure** 2.

The technical specifications of each ith follower are presented in **Table** 2. The controller sampling time is chosen as $T_d = 0.1\ s$. For this platoon configuration, *Theorem* 1 is solved to design a robust static output feedback controller for the longitudinal vehicle dynamics of each follower in the platoon. A feasible solution has been found using *MATLAB* LMI solvers. By setting $\gamma_y = 1$, a robust feasible control solution has been found with a minimum $\mathscr{H}_\infty$ performance index $\gamma_{opt} = 0.16$. These indexes guarantee that the platoon will be string stable, under **Theorem** 2.

In order to adapt the control input given to each follower according to the road conditions, the Kalman filter presented in **Section** IV is considered to estimate the longitudinal

TABLE 2. Parameters of each vehicle in the platoon.

i	m_i	τ_i	$C_{\omega i}$	Λ_i	f_{ri}
1	1546 kg	0.52 s	0.29	2.59 m^2	0.010
2	1994 kg	0.47 s	0.29	2.21 m^2	0.010
3	1916 kg	0.44 s	0.32	2.37 m^2	0.013
4	1406 kg	0.52 s	0.35	2.65 m^2	0.013
5	1034 kg	0.41 s	0.37	1.93 m^2	0.010

TABLE 3. Commercial sensor specifications.

Sensor	**Measured value**	**Accuracy**
Racelogic DGPS [46]	Vehicle position	$\pm$ 0.02 m
Racelogic Speed Sensors [46]	Vehicle speed	$\pm$ 0.1 km/h
Racelogic IMU [46]	Vehicle acceleration	$\pm$ 0.001 g

resistances. The measurement noise covariance and system noise covariance are set as:

$$\mathcal{R} = diag\{0.02^2, 0.027^2, 0.0098^2\},$$
$$\mathcal{Q} = diag\{0.1, 0.1, 5, 0.001\} \tag{32}$$

where the measurement noise covariance values are obtained from commercial sensor specifications listed in **Table** 3, and the system noise covariance is set by trial and error. The initial covariance of the states is also set as by trial and error:

$$\mathcal{P}_0 = diag\{0.1, 0.1, 0.5, 0.01\} \tag{33}$$

The desired separation between two neighboring vehicles is defined as $\delta_d = 10\ m$, alike similar works [26], [28], [43]. Furthermore, spacing, velocity and acceleration errors are initialized as zero, assuming that the heterogeneous platoon is in steady state before the simulation starts.

For comparison, the evaluation includes two control strategies:

1) A non-adaptive controller, designed under *Theorem* 1. The influence of external disturbances on the longitudinal dynamics of each follower is unknown, so the control input is not updated to compensate this effect.
2) An adaptive controller, designed under *Theorem* 1, which uses an estimator to compensate the effect of external disturbances on the longitudinal dynamics of the vehicle (see **Section** IV). **Proposed strategy.**

Furthermore, two simulation scenarios are created to test the driving performance of the platoon. The first scenario simulates highway traffic to approximate an everyday driving situation. The second scenario is designed to assess driving safety during a sudden brake on a downhill slope.

The simulations were performed using a computer equipped with an Intel Core i7-8700 CPU and 16 GB of memory under the MATLAB R2022b environment. As it suggested in the standard of SAE J2735 DSRC Message Set [47], the sampling frequency of the simulated measured and transmitted data among vehicles is set as 10 Hz [48].

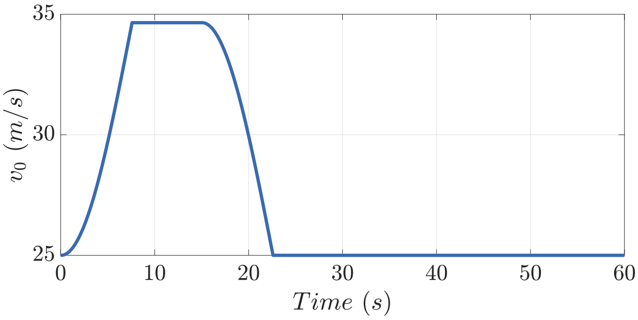

FIGURE 3. Leader speed profile used for scenario 1.

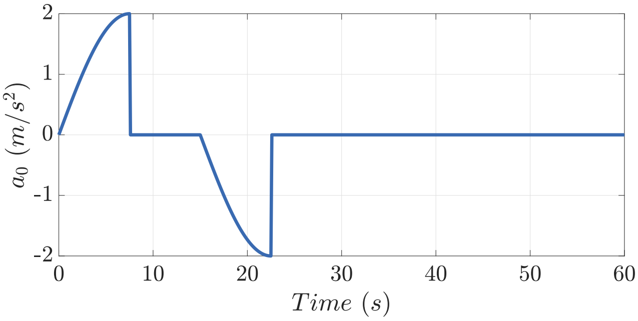

FIGURE 4. Leader acceleration profile used for scenario 1.

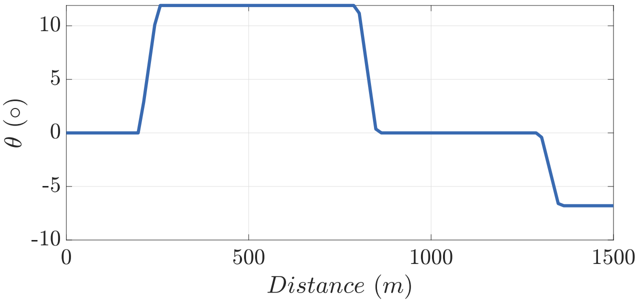

FIGURE 5. Road slope profile used for scenario 1.

A. SCENARIO 1. HIGHWAY TRAFFIC

The aim of this scenario is to examine the stability of the vehicle platoon as the velocity of the leader varies during highway movement. The leading vehicle follows the velocity and the acceleration profiles shown in **Figures** 3-4. The road slope considered for the simulation is depicted in **Figure** 5. The wind speed variation over time is shown in **Figure** 6.

From **Figures** 7 and 8, it is observed that the absolute values of the spacing error on the proposed architecture decreases when propagated downstream the platoon for the proposed case, i.e. $|\delta_1| > |\delta_2| > \cdots > |\delta_n|$, which proves the string stability of the vehicle platoon. Spacing errors are larger for the non-adaptive controller, which proves the necessity of estimating the effect of external disturbances on the vehicle. The maximum root mean square (RMS) spacing error for the adaptive controller is around 0.72 m, while the non-adaptive controller exceeds 1.39 m. Therefore,

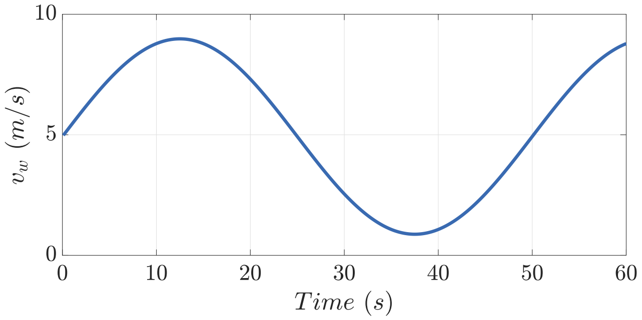

FIGURE 6. Wind speed profile used for scenario 1.

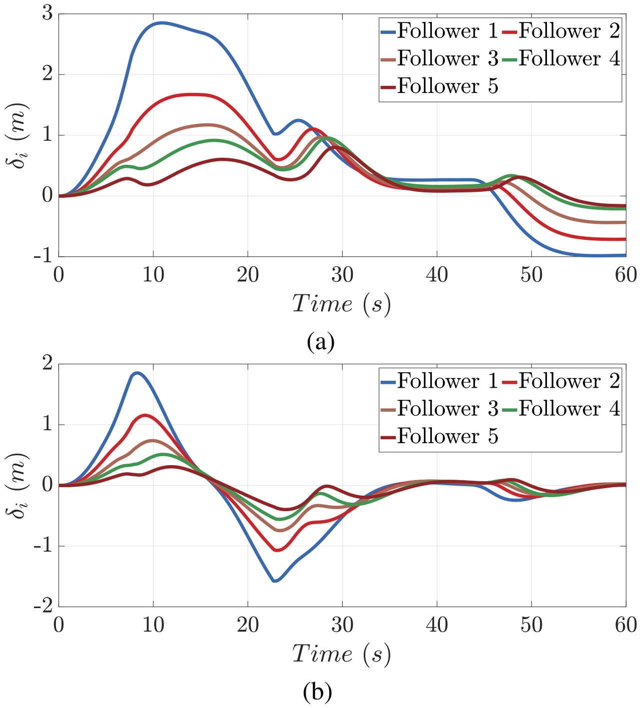

(a)

(b)

FIGURE 7. Spacing error evolution in the platoon for Scenario 1. (a) Non-adaptive controller. (b) Proposed controller.

a reduction of 48% in the spacing error is achieved by understanding how external disturbances affect the platoon.

Figures 9-10 show the evolution of followers' tracking velocity and acceleration over time. The results demonstrate that the proposed controller achieves steadier velocity and acceleration tracking compared to the non-adaptive controller, as the errors over time are lower for the proposed case. It is observed that the maximum velocity error is 0.64 m/s for the non-adaptive controller, while the proposed controller leads to a maximum velocity error of 0.43 m/s (32.8% reduction).

Figure 11 depicts the estimation of the external disturbances effect on the longitudinal dynamics of the first, middle and last follower. The actual effect of the disturbances on each vehicle in the platoon has been simulated following (4).

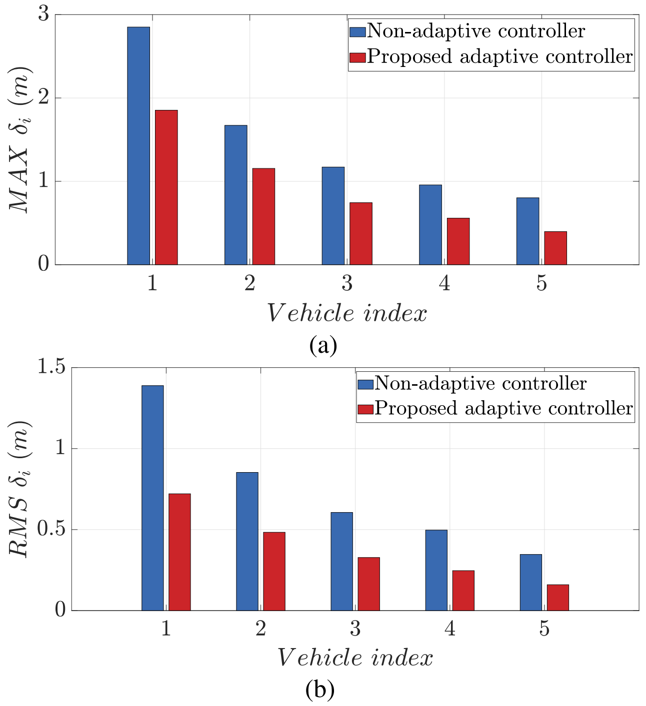

(a)

(b)

FIGURE 8. Spacing error for Scenario 1. (a) Max. (b) RMS.

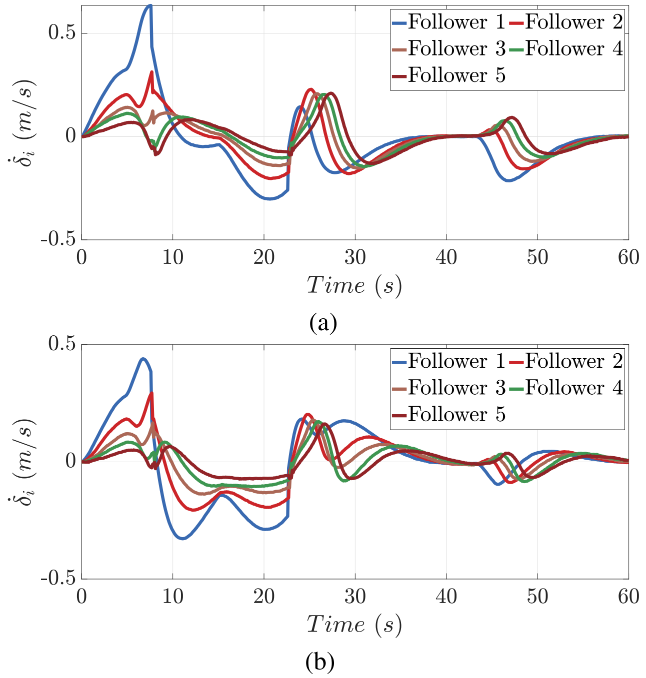

(a)

(b)

FIGURE 9. Velocity error evolution in the platoon for Scenario 1. (a) Non-adaptive controller. (b) Proposed controller.

The Kalman filter can precisely track how road profile, wind, and rolling resistance affect the longitudinal dynamics of each vehicle. This information is used to update the control input given to the engine to compensate for these effects.

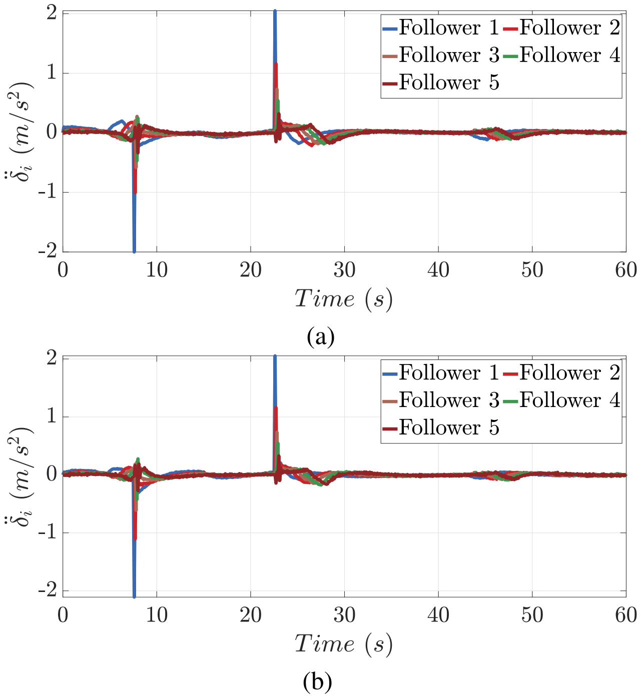

FIGURE 10. **Acceleration error evolution in the platoon for Scenario 1. (a) Non-adaptive controller. (b) Proposed controller.**

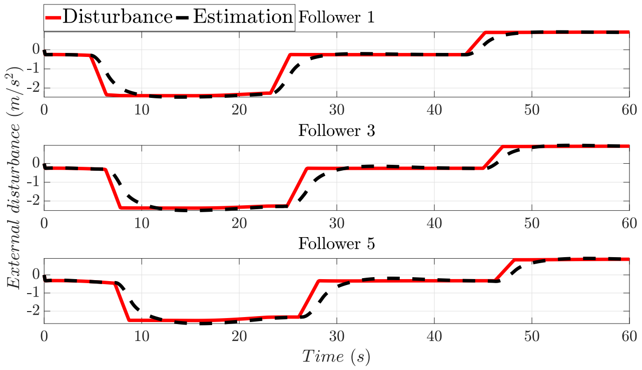

FIGURE 11. **Kalman filter performance for estimation of external disturbances.**

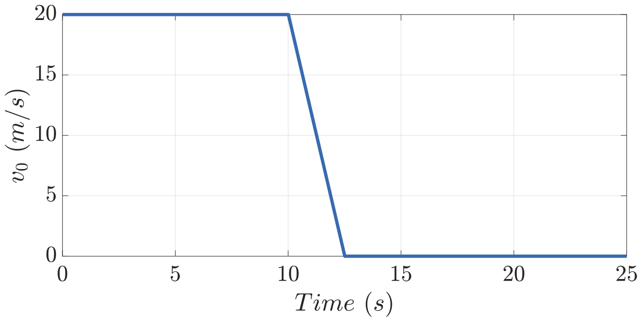

FIGURE 12. **Leader speed profile used for scenario 2.**

B. SCENARIO 2. EMERGENCY BRAKING ON A DOWNHILL SLOPE

This scenario evaluates the platoon's ability to perform an emergency braking maneuver under worst-case conditions for the road slope and wind. According to [43] and [44], the maximum road slope on hilly roads is 17°, while the wind speed during average driving conditions can reach velocities of up to 12.9 m/s. For this simulation, a constant wind speed of $v_w = 12.9\ m/s$ and road slope of $\theta = -17°$ are assumed. The leader velocity and acceleration profiles for this scenario are presented in **Figures** 12-13.

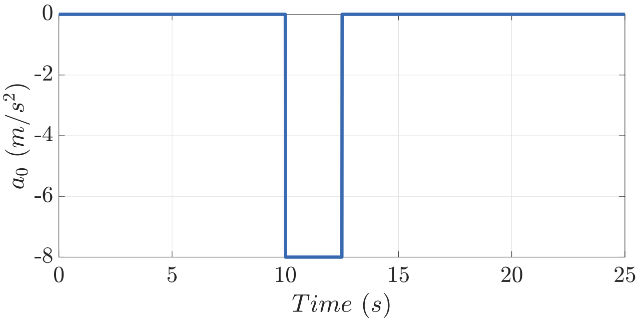

FIGURE 13. **Leader acceleration profile used for scenario 2.**

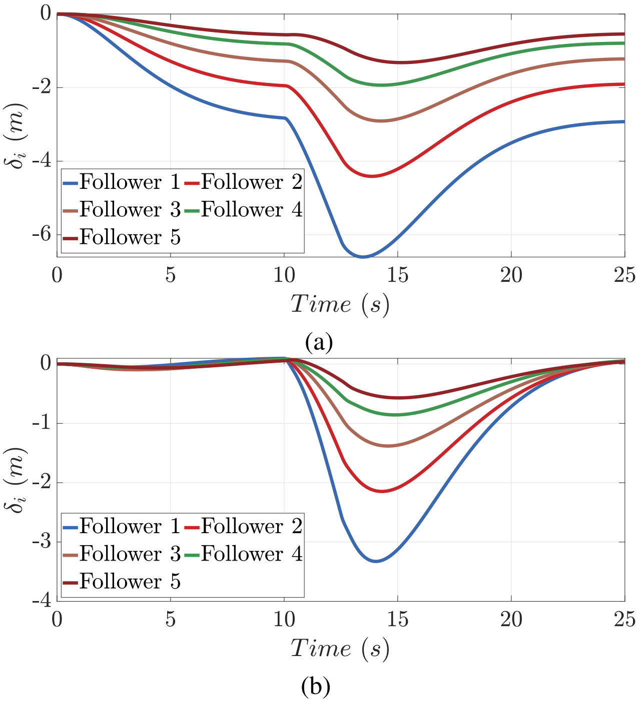

FIGURE 14. **Spacing error evolution in the platoon for Scenario 2. (a) Non-adaptive controller. (b) Proposed controller.**

The separation errors during this simulation are depicted in **Figures** 14 and 15. Although string stability is not compromised either for the proposed or the non-adaptive controller, transient errors increase when the controller does not compensate the effect of external disturbances on the platoon. The non-adaptive controller returns a maximum RMS separation error of 3.73 m, while with the proposed controller this value has decreased to 1.40 m (62.4% reduction). The maximum separation error between consecutive vehicles is found for the first follower, with a maximum separation error

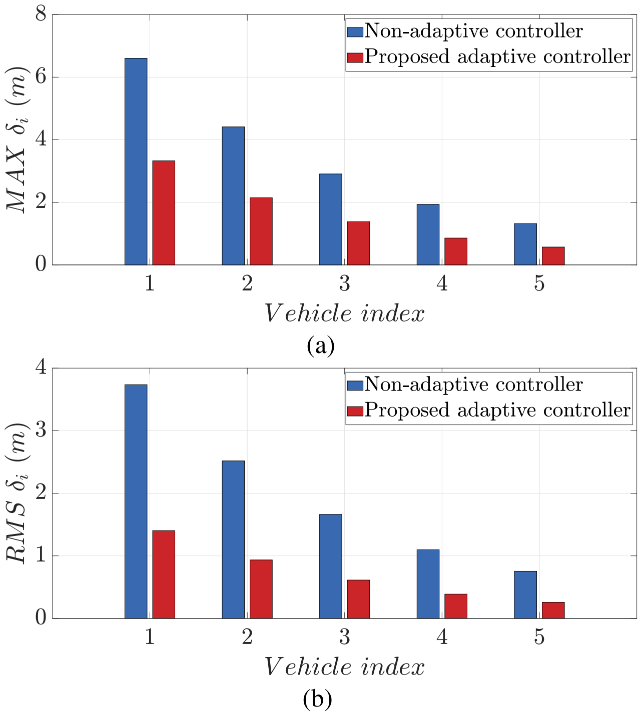

FIGURE 15. Spacing error for Scenario 2. (a) Max. (b) RMS.

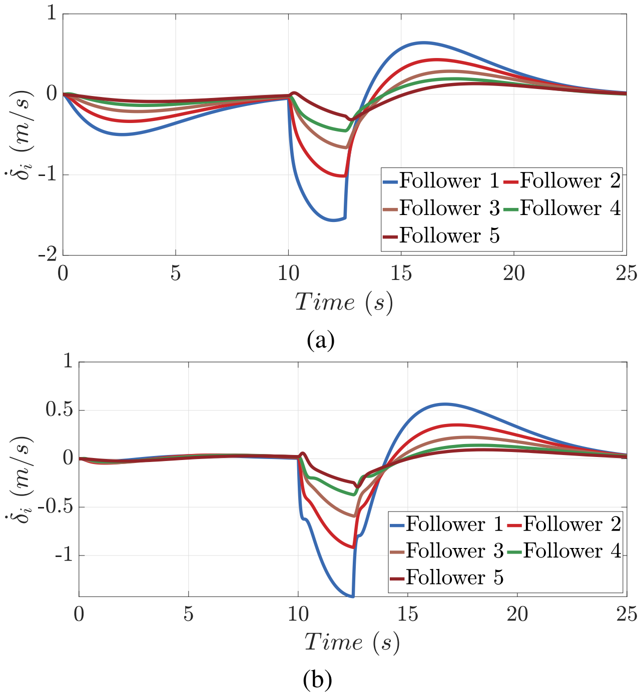

FIGURE 16. Velocity error evolution in the platoon for Scenario 2. (a) Non-adaptive controller. (b) Proposed controller.

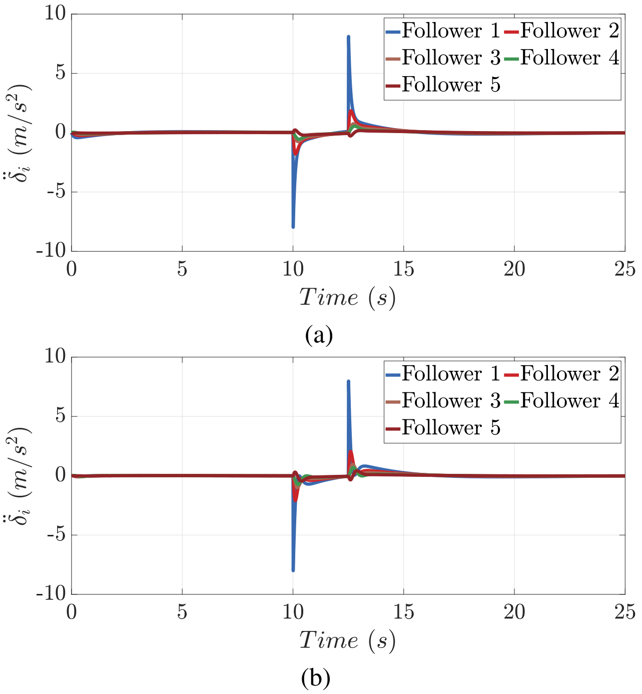

FIGURE 17. Acceleration error evolution in the platoon for Scenario 2. (a) Non-adaptive controller. (b) Proposed controller.

of 6.60 m for the non-adaptive controller. Remembering that $\delta_d = 10\ m$, this follower is only 3.4 m far from the preceding vehicle. For the proposed controller, the maximum separation error is 3.32 m, which means that it is 6.68 m away from the preceding vehicle. This proves that the proposed controller ensures safer driving conditions.

Figures 16-17 present the velocity and acceleration errors for this simulations. The proposed controller achieves a more smooth leader following behavior, with a maximum velocity tracking error of 1.42 m/s, compared to the 1.53 m/s error found for the non-adaptive controller.

VI. CONCLUSION

This paper has presented an investigation of the problem of robust heterogeneous vehicle platoon control while estimating and compensating the effect of disturbances on the longitudinal dynamics of each vehicle.

The platoon design is performed in the discrete-time domain in order to facilitate the real-time implementation. System stability is guaranteed under Lyapunov criteria. $\mathscr{H}_\infty$ norm is analyzed to study the robustness of the proposed strategy towards external disturbances and measurement noise.

A Kalman filter is considered to estimate and compensate the effect of external disturbances such as aerodynamic drag, rolling resistance and gravitational resistance on the longitudinal dynamics of each follower vehicle.

The proposed method achieves a more smooth and safer platoon following performance compared to a non-adaptive strategy. String stability is guaranteed since spacing errors tend to decrease when propagated along the platoon. The spacing error is reduced in the platoon with over 62% spacing error reduction for worst cases when compared to the non-adaptive strategy.

The results demonstrate the effectiveness of the proposed system in emergency braking maneuvers, doubling the safety distance with the preceding vehicle compared to a controller that does not consider the effect of road slope or wind on the vehicle. The aforementioned conclusions serve to reinforce the interest of implementing the proposed control approach in a real vehicle platoon. This is expected to enhance road safety and reduce traffic congestion.

Future research will investigate the effects of communication delays, interruptions, and failures on a vehicle platoon. Additionally, the lateral movement of the platoon will be performed by a path tracking controller. In this case, it will be necessary to evaluate how lateral wind affects the vehicle motion.

REFERENCES

[1] Ê. Vasconcelos Filho, R. Severino, P. M. Salgueiro dos Santos, A. Koubaa, and E. Tovar, "Cooperative vehicular platooning: A multi-dimensional survey towards enhanced safety, security and validation," *Cyber-Phys. Syst.*, vol. 1, pp. 1–53, Jun. 2023.

[2] W. N. Caballero, D. Rios Insua, and R. Naveiro, "Some statistical challenges in automated driving systems," *Appl. Stochastic Models Bus. Ind.*, vol. 39, no. 5, pp. 629–652, Sep. 2023.

[3] F. Viadero-Monasterio, J. García, M. Meléndez-Useros, M. Jiménez-Salas, B. L. Boada, and M. J. López Boada, "Simultaneous estimation of vehicle sideslip and roll angles using an event-triggered-based IoT architecture," *Machines*, vol. 12, no. 1, p. 53, Jan. 2024.

[4] S. Yang, Y. Huang, L. Li, S. Feng, X. Na, H. Chen, and A. Khajepour, "How to guarantee driving safety for autonomous vehicles in a real-world environment: A perspective on self-evolution mechanisms," *IEEE Intell. Transp. Syst. Mag.*, vol. 16, no. 2, pp. 41–54, Mar. 2024.

[5] L. Zhang, W.-W. Che, S. Xu, and C. Deng, "Prescribed performance tracking control for 2-D plane vehicle platoons with actuator faults and saturations," *IEEE Trans. Veh. Technol.*, vol. 72, no. 11, pp. 14040–14050, Nov. 2023.

[6] S. Feng, Y. Zhang, S. E. Li, Z. Cao, H. X. Liu, and L. Li, "String stability for vehicular platoon control: Definitions and analysis methods," *Annu. Rev. Control*, vol. 47, pp. 81–97, Oct. 2019.

[7] Y. Xue, X. Zhang, Z. Cui, B. Yu, and K. Gao, "A platoon-based cooperative optimal control for connected autonomous vehicles at highway on-ramps under heavy traffic," *Transp. Res. Part C, Emerg. Technol.*, vol. 150, May 2023, Art. no. 104083.

[8] F. Viadero-Monasterio, M. Meléndez-Useros, M. Jiménez-Salas, B. L. Boada, and M. J. L. Boada, "What are the most influential factors in a vehicle platoon?" in *Proc. IEEE Int. Conf. Evolving Adapt. Intell. Syst. (EAIS)*, May 2024, pp. 1–7.

[9] A. Khalil, M. A. Janaideh, and D. Kundur, "Online fault classification in connected autonomous vehicles using output-only measurements," *Mech. Syst. Signal Process.*, vol. 190, May 2023, Art. no. 110099.

[10] G. Liu, R. Zhao, and M. Su, "Cooperative adaptive sliding mode platoon control of intelligent connected vehicles under communication interruption," *Int. J. Automot. Technol.*, vol. 24, no. 2, pp. 513–525, 2023.

[11] A. Khalifa, O. Kermorgant, S. Dominguez, and P. Martinet, "Platooning of car-like vehicles in urban environments: Longitudinal control considering actuator dynamics, time delays, and limited communication capabilities," *IEEE Trans. Control Syst. Technol.*, vol. 29, no. 6, pp. 2670–2677, Nov. 2021.

[12] Y. Lin, A. Tiwari, B. Fabien, and S. Devasia, "Constant-spacing connected platoons with robustness to communication delays," *IEEE Trans. Intell. Transp. Syst.*, vol. 24, no. 3, pp. 3370–3382, Mar. 2023.

[13] L. Xiao and F. Gao, "A comprehensive review of the development of adaptive cruise control systems," *Vehicle Syst. Dyn.*, vol. 48, no. 10, pp. 1167–1192, Oct. 2010.

[14] Y. Dai, C. Wang, and Y. Xie, "Explicitly incorporating surrogate safety measures into connected and automated vehicle longitudinal control objectives for enhancing platoon safety," *Accident Anal. Prevention*, vol. 183, Apr. 2023, Art. no. 106975.

[15] P. Zhu, S. Jin, X. Bu, and Z. Hou, "Distributed data-driven control for a connected heterogeneous vehicle platoon under quantized and switching topologies communication," *IEEE Trans. Veh. Technol.*, vol. 72, no. 8, pp. 9796–9807, Aug. 2023.

[16] Z. Liu, Z. Li, G. Guo, and H. Cheng, "Cooperative platoon control of heterogeneous vehicles under a novel event-triggered communication strategy," *IEEE Access*, vol. 7, pp. 41172–41182, 2019.

[17] A. Bayuwindra, L. Wonohito, and B. R. Trilaksono, "Design of DDPG-based extended look-ahead for longitudinal and lateral control of vehicle platoon," *IEEE Access*, vol. 11, pp. 96648–96660, 2023.

[18] L. Xu, W. Zhuang, G. Yin, and C. Bian, "Distributed formation control of homogeneous vehicle platoon considering vehicle dynamics," *Int. J. Automot. Technol.*, vol. 20, no. 6, pp. 1103–1112, Dec. 2019.

[19] L. Xu, W. Zhuang, G. Yin, and C. Bian, "Energy-oriented cruising strategy design of vehicle platoon considering communication delay and disturbance," *Transp. Res. Part C, Emerg. Technol.*, vol. 107, pp. 34–53, Oct. 2019.

[20] F. I. Villenas, F. J. Vargas, and A. A. Peters, "A Kalman-based compensation strategy for platoons subject to data loss: Numerical and empirical study," *Mathematics*, vol. 11, no. 5, p. 1228, Mar. 2023.

[21] T. Yang, C. Murguia, D. Nesic, and C. Lv, "A robust CACC scheme against cyberattacks via multiple vehicle-to-vehicle networks," *IEEE Trans. Veh. Technol.*, vol. 72, no. 9, pp. 11184–11195, Sep. 2023.

[22] M. R. Hidayatullah and J.-C. Juang, "Centralized and distributed control framework under homogeneous and heterogeneous platoon," *IEEE Access*, vol. 9, pp. 49629–49648, 2021.

[23] X. Mao, P. Li, Z. Weng, and J. Zhao, "Distributed tube model predictive control for string stability of heterogeneous vehicle platoons," *Proc. Inst. Mech. Eng., I, J. Syst. Control Eng.*, vol. 237, no. 10, pp. 1777–1788, Nov. 2023.

[24] J. Wang, X. Luo, Y. Zhang, and X. Guan, "Distributed integrated sliding mode control via neural network and disturbance observer for heterogeneous vehicle systems with uncertainties," *Trans. Inst. Meas. Control*, vol. 45, no. 11, pp. 2204–2215, Jul. 2023.

[25] G. Na, G. Park, V. Turri, K. H. Johansson, H. Shim, and Y. Eun, "Disturbance observer approach for fuel-efficient heavy-duty vehicle platooning," *Vehicle Syst. Dyn.*, vol. 58, no. 5, pp. 748–767, May 2020.

[26] J. Chen, H. Zhang, and G. Yin, "Distributed dynamic event-triggered secure model predictive control of vehicle platoon against DoS attacks," *IEEE Trans. Veh. Technol.*, vol. 72, no. 3, pp. 2863–2877, Mar. 2023.

[27] P. Wang, H. Deng, J. Zhang, L. Wang, M. Zhang, and Y. Li, "Model predictive control for connected vehicle platoon under switching communication topology," *IEEE Trans. Intell. Transp. Syst.*, vol. 23, no. 7, pp. 7817–7830, Jul. 2022.

[28] L. Xu, W. Zhuang, G. Yin, and C. Bian, "Stable longitudinal control of heterogeneous vehicular platoon with disturbances and information delays," *IEEE Access*, vol. 6, pp. 69794–69806, 2018.

[29] Z. Tang, L. Xu, G. Yin, and H. Liu, "L_2 string stability of heterogeneous platoon under disturbances and information delays," in *Proc. Chin. Control Decis. Conf. (CCDC)*, Jun. 2019, pp. 5472–5477.

[30] Z. Wu, J. Sun, and S. Hong, "RBFNN-based adaptive event-triggered control for heterogeneous vehicle platoon consensus," *IEEE Trans. Intell. Transp. Syst.*, vol. 23, no. 10, pp. 18761–18773, Oct. 2022.

[31] Y. Liu, L. Wei, Z. Fan, X. Wang, and L. Li, "Road slope estimation based on acceleration adaptive interactive multiple model algorithm for commercial vehicles," *Mech. Syst. Signal Process.*, vol. 184, Feb. 2023, Art. no. 109733.

[32] S. M. Moradi, A. Akbari, and M. Mirzaei, "An offline LMI-based robust model predictive control of vehicle active suspension system with parameter uncertainty," *Trans. Inst. Meas. Control*, vol. 41, no. 6, pp. 1699–1711, Apr. 2019.

[33] R. Jin, P. Rocco, X. Chen, and Y. Geng, "LPV-based offline model predictive control for free-floating space robots," *IEEE Trans. Aerosp. Electron. Syst.*, vol. 57, no. 6, pp. 3896–3904, Dec. 2021.

[34] G. Bellegarda and Q. Nguyen, "Dynamic vehicle drifting with nonlinear MPC and a fused kinematic-dynamic bicycle model," *IEEE Control Syst. Lett.*, vol. 6, pp. 1958–1963, Dec. 2021.

[35] F. Viadero-Monasterio, A.-T. Nguyen, J. Lauber, M. J. L. Boada, and B. L. Boada, "Event-triggered robust path tracking control considering roll stability under network-induced delays for autonomous vehicles," *IEEE Trans. Intell. Transp. Syst.*, vol. 24, no. 12, pp. 14743–14756, Dec. 2023.

[36] Y. Zhao, Z. Liu, and W. S. Wong, "Resilient platoon control of vehicular cyber physical systems under DoS attacks and multiple disturbances," *IEEE Trans. Intell. Transp. Syst.*, vol. 23, no. 8, pp. 10945–10956, Aug. 2022.

[37] F. Viadero-Monasterio, B. Boada, M. Boada, and V. Díaz, "H_∞dynamic output feedback control for a networked control active suspension system under actuator faults," *Mech. Syst. Signal Process.*, vol. 162, Aug. 2022, Art. no. 108050.

[38] C. K. Yuksel, J. Busek, M. Anderle, T. Vyhlídal, and S.-I. Niculescu, "A distributed delay based controller for simultaneous periodic disturbance rejection and input-delay compensation," *Mech. Syst. Signal Process.*, vol. 197, Aug. 2023, Art. no. 110364.

[39] F. Viadero-Monasterio, B. L. Boada, H. Zhang, and M. J. L. Boada, "Integral-based event triggering actuator fault-tolerant control for an active suspension system under a networked communication scheme," *IEEE Trans. Veh. Technol.*, vol. 72, no. 11, pp. 13848–13860, Nov. 2023.

[40] H. Guo, J. Guo, X. Zhao, D. Cao, H. Chen, and S. Yu, "Data-mechanism adaptive switched predictive control for heterogeneous platoons with wireless communication interruption," *IEEE Trans. Intell. Transp. Syst.*, vol. 24, no. 10, pp. 10553–10571, Oct. 2023.

[41] Q. Xia, F. Gao, J. Duan, and Y. He, "Decoupled H_∞ control of automated vehicular platoons with complex interaction topologies," *IET Intell. Transp. Syst.*, vol. 11, no. 2, pp. 92–101, Mar. 2017.

[42] G. Guo, P. Li, and L.-Y. Hao, "A new quadratic spacing policy and adaptive fault-tolerant platooning with actuator saturation," *IEEE Trans. Intell. Transp. Syst.*, vol. 23, no. 2, pp. 1200–1212, Feb. 2022.

[43] F. Gao, S. E. Li, Y. Zheng, and D. Kum, "Robust control of heterogeneous vehicular platoon with uncertain dynamics and communication delay," *IET Intell. Transp. Syst.*, vol. 10, no. 7, pp. 503–513, Sep. 2016.

[44] R. Rajamani, *Vehicle Dynamics and Control*. Cham, Switzerland: Springer, 2011.

[45] M. Meléndez-Useros, M. Jiménez-Salas, F. Viadero-Monasterio, and B. L. Boada, "Tire slip H_∞ control for optimal braking depending on road condition," *Sensors*, vol. 23, no. 3, p. 1417, Jan. 2023.

[46] Racelogic. *Sensors*. Accessed: Jan. 22, 2024. [Online]. Available: https://en.racelogic.support/VBOX_Automotive/Product_Info/Sensors

[47] J. B. Kenney, "Dedicated short range communications (DSRC) message set dictionary," *Proc. IEEE*, vol. 16, no. 7, pp. 1162–1182, 2016.

[48] F. Ma, J. Wang, S. Zhu, S. Y. Gelbal, Y. Yang, B. Aksun-Guvenc, and L. Guvenc, "Distributed control of cooperative vehicular platoon with nonideal communication condition," *IEEE Trans. Veh. Technol.*, vol. 69, no. 8, pp. 8207–8220, Aug. 2020.

FERNANDO VIADERO-MONASTERIO (Member, IEEE) received the B.S. degree in industrial engineering from the Universidad de Cantabria (UNICAN), Santander, Spain, in 2018, and the M.S. degree in industrial engineering and the Ph.D. degree in mechanical engineering from the University Carlos III de Madrid (UC3M), Madrid, Spain, in 2020 and 2023, respectively. He joined the Department of Mechanical Engineering, UC3M, in 2018. His research interests include vehicle dynamics, vehicle safety, control systems, fault-tolerant control, and non-linear systems. He is a member of IFToMM Technical Committee for Transportation Machinery.

MIGUEL MELÉNDEZ-USEROS (Graduate Student Member, IEEE) received the B.S. and M.S. degrees in industrial engineering from the Universidad Carlos III de Madrid (UC3M), Madrid, Spain, in 2020 and 2022, respectively, where he is currently pursuing the Ph.D. degree. He joined the Department of Mechanical Engineering, UC3M, in 2020. His research interests include vehicle dynamics, vehicle safety, control systems, and fault-tolerant control and fault detection.

MANUEL JIMÉNEZ-SALAS (Graduate Student Member, IEEE) received the B.S. degree in industrial engineering from the Universidad de Malaga (UMA), Malaga, Spain, in 2019, and the M.S. degree in industrial engineering from the Universidad Carlos III de Madrid (UC3M), Madrid, Spain, in 2021, where he is currently pursuing the Ph.D. degree. He joined the Department of Mechanical Engineering, UC3M, in 2019. His research interests include vehicle dynamics, vehicle safety, control systems, and path following control.

BEATRIZ L. BOADA received the degree in industrial engineering and the Ph.D. degree from the Universidad Carlos III de Madrid (UC3M), Madrid, Spain, in 1996 and 2002, respectively. From 1997 to 2002, she was a Research Assistant with the Department of Systems and Automation Engineering, UC3M. She was with localization and mapping problems in the field of robotic. She is currently a Full Professor with the Mechanical Engineering Department, UC3M. Since 2017, she has been co-responsible of the Research Group Experimental Mechanics, Calculations and Transport. Her research interests include intelligent vehicles, both autonomous and motorized and control of vehicle in vertical, lateral dynamics, magnetorheological dampers, uncertainties modeling, and estimation of mechanical systems.